Equilibration Dynamics of Strongly Interacting Bosons in 2D Lattices with Disorder

Mi Yan,[1] Hoi-Yin Hui,[1] Marcos Rigol,[2] and Vito W. Scarola[1]

[1] *Department of Physics, Virginia Tech, Blacksburg, VA 24061, USA*
[2] *Department of Physics, The Pennsylvania State University, University Park, PA 16802, USA*

(Dated: June 13, 2016)

Motivated by recent optical lattice experiments [Choi et al., arXiv:1604.04178], we study the dynamics of strongly interacting bosons in the presence of disorder in two dimensions. We show that Gutzwiller mean-field theory (GMFT) captures the main experimental observations, which are a result of the competition between disorder and interactions. Our findings highlight the difficulty in distinguishing glassy dynamics, which can be captured by GMFT, and many-body localization, which cannot be captured by GMFT, and indicate the need for further experimental studies of this system.

PACS numbers: 67.85.-d, 05.30.Jp, 72.15.Rn, 05.70.Ln

Introduction: Ultracold atoms loaded into optical lattices [1–3] offer ideal platforms to study localization [4, 5]. Examples in the noninteracting limit include fermionic band insulators [6], and, in the presence of (quasi-)disorder, Anderson insulators [7–12]. In clean systems, localization can also occur because of interactions, which can produce Mott insulating phases [13–17]. Recent experimental studies have started exploring the interplay between disorder and interactions [18–28]. In the ground state of bosonic systems, this interplay can generate a phase known as the Bose-glass [29, 30]. The Bose-glass, like the bosonic Mott insulator, is characterized by a vanishing superfluid density but, unlike the Mott insulator, it is compressible. At extensive energy densities above the ground state, the interplay between disorder and interactions can lead to a remarkable phenomenon known as many-body localization (MBL) [31–33]. In the MBL phase, eigenstate thermalization [34–36], and as a result thermalization, do not occur [37].

Signatures of MBL were recently observed with fermions [26, 27] and bosons in two dimensions (2D) [28]. Our work is motivated by the latter experiment (see Refs. [38, 39] for theoretical studies inspired by the former). In Ref. [28], a Mott insulating state with one boson per site was prepared in a harmonic trap in a very deep optical lattice. All bosons in one half of the system were then removed and the remaining half was allowed to evolve by lowering the lattice depth, in the absence or presence of disorder. During the dynamics, the parity projected occupation of the lattice sites was measured using fluorescence imaging, allowing the study of the evolution of the imbalance $\mathcal{I}$ between the initially occupied and unoccupied halves of the system. In the absence of disorder, or for weak disorder, $\mathcal{I}$ vanished within times accessible experimentally, i.e., it attained the value expected in thermal equilibrium. But beyond a certain disorder strength, $\mathcal{I}$ appeared to saturate to a nonzero value. This saturation was taken as evidence for MBL [28].

Features of the experimental setup in Ref. [28] can lead to a very slow equilibration of $\mathcal{I}$ to the point of making it very difficult to distinguish the ergodic from the MBL phase. First, the initial dynamics in the unoccupied half of the trap is dominated by Anderson physics (because of low site occupation). The second feature sets in at longer times. We note that the initial Mott insulator, before the removal of the bosons in one half of the system, is close in energy to the ground state after the lattice depth is lowered but the system remains deep in the Mott regime. The latter, in turn, is close in energy to a Bose-glass with a site occupancy slightly below one at the same interaction strength (if the disorder is strong enough to generate a Bose-glass). As a result, the dynamics resulting from the gradual decrease of the site occupations in the occupied half of the system, after the removal of the bosons in the other half, can be dominated by Bose-glass physics.

To study the impact of glassy physics we use Gutzwiller mean-field theory (GMFT) to model the dynamics of the experimental setup in Ref. [28]. GMFT is known to provide qualitatively correct phase diagrams for strongly interacting clean [40–43] and disordered [44–48] (away from the tip of the Mott lobe) systems. It has also been used to study nonequilibrium effects such as the dynamical generation of molecular condensates [49] and Mott insulators [50], dipole oscillations [51], quantum quenches [48, 52, 53], expansion dynamics [54, 55], and transport in the presence of disorder [48, 56]. However, since the Gutzwiller ansatz wavefunction is a product state, it has zero entanglement entropy for any partitioning of the system. GMFT is therefore not suited to describe thermalization and MBL phases [57], which after taken out of equilibrium, e.g., using a quantum quench, exhibit a linear [58] and logarithmic [59] growth of the entanglement entropy, respectively, with time.

We study the dynamics of three initial states under the same (or similar) final conditions as the experiment. The first initial state is the same (within GMFT) as in the experiment, the second one has lower site occupancies to show how a superfluid/Bose-glass evolves under similar conditions, and the third one is devised to enhance the effects of interactions. We show that the dynamics of those initial states is qualitatively similar to the one observed experimentally, while quantitative differences do occur. Given the fact that GMFT cannot describe dy-

namics in an MBL phase, our results raise concerns as to whether what was observed experimentally is the result of MBL or the result of slow transport due to glassy dynamics. Only the latter is qualitatively captured by our GMFT treatment.

Model: We consider bosons in a 2D square lattice subjected to disorder and a parabolic trapping potential, as described by the Bose-Hubbard Hamiltonian:

$$\hat{H} = -J\sum_{\langle \mathbf{ij}\rangle} \hat{b}_{\mathbf{i}}^{\dagger}\hat{b}_{\mathbf{j}} + \frac{U}{2}\sum_{\mathbf{i}} \hat{n}_{\mathbf{i}}\left(\hat{n}_{\mathbf{i}}-1\right) + \sum_{\mathbf{i}} \mu_{\mathbf{i}}\hat{n}_{\mathbf{i}}, \quad (1)$$

where $\hat{b}_{\mathbf{i}}^{\dagger}$ creates a boson at site $\mathbf{i} \equiv (i_x, i_y)$ and $\hat{n}_{\mathbf{i}} = \hat{b}_{\mathbf{i}}^{\dagger}\hat{b}_{\mathbf{i}}$ is the site occupation operator. J parametrizes the tunneling between nearest-neighbor sites and U is the on-site repulsive interaction. The chemical potential (μ), harmonic trap (of strength Ω), and disorder potential ($\epsilon_{\mathbf{i}}$) are accounted for in $\mu_{\mathbf{i}} = -\mu + \Omega\left|\mathbf{i}-\mathbf{r}_0\right|^2 + \epsilon_{\mathbf{i}}$, with $\mathbf{r}_0 = (1/2, 1/2)$ to place the center of the trap at the middle of a 4-site plaquette. We focus on a lattice with 32×32 sites in which, for the Hamiltonian parameters used here, the sites at the edges are always empty. We consider two types of disorder, uniform and Gaussian distributed, whose strengths are denoted by Δ_u and Δ_g, respectively. In what follows, we set $k_B = \hbar = 1$.

Methods: We study the dynamics of zero and nonzero temperature initial states. The density matrix within GMFT is:

$$\hat{\rho}\left(t\right) = \prod_{\mathbf{i}} \hat{\rho}_{\mathbf{i}}\left(t\right) = \prod_{\mathbf{i}} \left[\sum_{m,n=0}^{\infty} \alpha_{mn}^{(\mathbf{i})}\left(t\right)\left|m\right\rangle_{\mathbf{i}}\ {}_{\mathbf{i}}\left\langle n\right|\right], \quad (2)$$

where $|n\rangle_{\mathbf{i}}$ is the state with n bosons at site $\mathbf{i}$, and t is time. This ansatz decouples Eq. (1) into single-site Hamiltonians of the form $\hat{H}_{\mathbf{i}}^{\mathrm{MF}} = -J(\phi_{\mathbf{i}}^{*}\hat{b}_{\mathbf{i}} + \phi_{\mathbf{i}}\hat{b}_{\mathbf{i}}^{\dagger}) + (U/2)\sum_{\mathbf{i}}\hat{n}_{\mathbf{i}}(\hat{n}_{\mathbf{i}}-1) + \mu_{\mathbf{i}}\hat{n}_{\mathbf{i}}$, where $\phi_{\mathbf{i}} = \sum_{\mathbf{j}\in \mathrm{nn}_{\mathbf{i}}} \mathrm{Tr}(\hat{\rho}_{\mathbf{j}}\hat{b}_{\mathbf{j}})$ sums over neighbor sites to $\mathbf{i}$. Substituting Eq. (2) into the von Neumann equation, $i\partial_t\hat{\rho} = [\hat{H}, \hat{\rho}]$, leads to the equation of motion for $\alpha_{mn}^{(\mathbf{i})}$:

$$\begin{aligned} i\partial_t \alpha_{m,n}^{(\mathbf{i})} = &-J\phi_{\mathbf{i}}^{*}\left[\sqrt{m+1}\,\alpha_{m+1,n}^{(\mathbf{i})} - \sqrt{n}\,\alpha_{m,n-1}^{(\mathbf{i})}\right] \\ &-J\phi_{\mathbf{i}}\left[\sqrt{m}\,\alpha_{m-1,n}^{(\mathbf{i})} - \sqrt{n+1}\,\alpha_{m,n+1}^{(\mathbf{i})}\right] \\ &+\frac{U}{2}\left[m\left(m-1\right) - n\left(n-1\right)\right]\alpha_{m,n}^{(\mathbf{i})} \\ &+\mu_{\mathbf{i}}\left(m-n\right)\alpha_{m,n}^{(\mathbf{i})}, \end{aligned} \quad (3)$$

which yields the time evolution of the site occupations: $n_{\mathbf{i}}(t) = \mathrm{Tr}(\hat{\rho}_{\mathbf{i}}\hat{n}_{\mathbf{i}})$.

Following Ref. [28], we quantify the degree of localization using the imbalance:

$$\mathcal{I}(t) = \frac{N_L(t) - N_R(t)}{N_L(t) + N_R(t)}, \quad (4)$$

where $N_L(t) = \sum_{i_x\leq 0, |i_y-\frac{1}{2}|<3} n_{i_x,i_y}(t)$ and $N_R(t) = \sum_{i_x>0, |i_y-\frac{1}{2}|<3} n_{i_x,i_y}(t)$. We also compute the inverse decay length λ at time t [28]. To calculate $\lambda(t)$ we first compute the average: $\bar{n}_{i_x}(t) = (1/6)\sum_{|i_y-\frac{1}{2}|<3} n_{i_x,i_y}(t)$. λ is then obtained by fitting:

$$\bar{n}_{i_x}\left(t\right)/\bar{n}_{i_x}^{0} \sim e^{-\lambda(t)\, i_x}, \quad (5)$$

where $\bar{n}_{i_x}^{0}$ is the zero disorder steady-state density.

For $\hat{\rho}\left(t=0\right)$, we take the ground state or a thermal state of the initial Hamiltonian, such that $\hat{\rho}_{\mathbf{i}} = Z_{\mathbf{i}}^{-1}e^{-\beta\hat{H}_{\mathbf{i}}^{\mathrm{MF}}}$ (where $\beta = 1/T$ is the inverse temperature and $Z_{\mathbf{i}}$ is the partition function). The computation of $\phi_{\mathbf{i}}$ and $\hat{\rho}_{\mathbf{i}}$ is done iteratively until convergence, and is carried out for several initial trials of $\phi_{\mathbf{i}}$. The state with the lowest free energy is the one used for the dynamics. Our calculations for finite disorder are done for an ensemble of disorder realizations. Disorder-averaging over around 100 disorder realizations is sufficient for convergence.

It is important to stress that, within GMFT, dynamics occur only when there are nonvanishing values of the order parameter $\phi_{\mathbf{i}}$ [see Eq. (3)] in the initial state. As a result, a pure Mott insulating state would exhibit no dynamics within this approximation. We find that, as in Refs. [55, 56], the small region with a non-vanishing order parameter generated by the harmonic trap at the edge of Mott insulating domains is sufficient to drive dynamics for the parameters considered here. Remarkably, the ensuing dynamics is qualitatively similar to that in

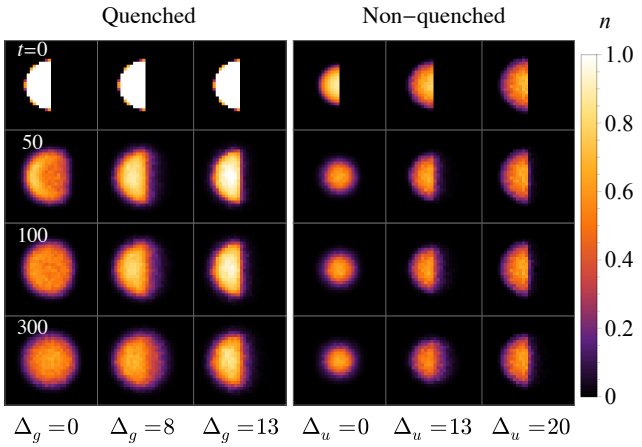

Figure 1. Snapshots of the site occupations for the quenched (left panel) and non-quenched (right panel) dynamics at zero temperature. Columns (rows) depict results for different disorder strengths (different times). At time $t = 0$ all bosons in the right half of the system are removed and the remainder evolves for $t > 0$. Quenched: The $t = 0$ state is the ground state for a very small value of the hopping parameter and no disorder. For $t > 0$, Gaussian disorder of strength Δ_g is introduced and the hopping parameter is set to a larger value. The evolution is studied without further parameter changes (the same parameters as in Ref. [28], see text). Non-quenched case: The initial state is the ground state for the same values of U, J, and Ω as those in Ref. [28] after the quench. The state evolves for $t \geq 0$ with no parameter changes. The initial site occupations allow a superfluid or a Bose-glass depending on the strength of the uniformly distributed disorder, Δ_u.

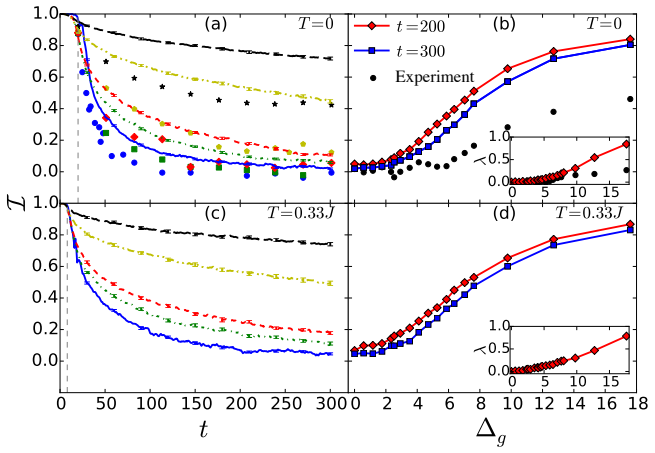

Figure 2. (a) and (c): Time evolution of the imbalance $\mathcal{I}$ for various disorder strengths when the initial temperature is $T = 0$ (a) and $T = 0.33$ (c). Lines show simulation results while points show the corresponding experimental data from Ref. [28]. The vertical dashed line marks a time t^* ($t^* = 20$ for $T = 0$ and $t^* = 8$ for $T = 0.33$) below which $\mathcal{I}$ almost does not change within GMFT. t^* is an artifact of GMFT for the initial state selected. The experimental results are shifted to start at t^*. From bottom to top the lines and symbols correspond to $\Delta_g = 0, 3, 4, 8$, and 13. (b) and (d): Corresponding $\mathcal{I}$ for the same parameters but at times $t = 200$ and 300 against disorder strength. The experimental result after an evolution time of 187 are also plotted. The inset shows the inverse decay length [Eq. (5)] from our calculation at $t = 200$ and for the experiment after an evolution time $t = 187$.

the experiments [28], especially at long times.

Quenched case: In the experiment [28] the dynamics took place after lowering the lattice depth and introducing a disorder potential to a Mott insulator created in a very deep lattice and to which all atoms in one half of the system were removed. To distinguish it from other protocols discussed later, we refer to this case as the "quenched case". From now on, we use the hopping parameter after the quench $J_F = U/24.4$ as our energy unit. To create the initial state we used the experimental parameters [28]: $J_I = 0.244$, $U = 24.4$, $\Omega = 0.145$, and $\mu = 10.6$. After the free energy minimization, the particles on the right half of the system are manually removed [by setting $\alpha_{m,n}^{(i_x>0)} = \delta_{m,0}\delta_{n,0}$ in Eq. (2)], leaving behind a number of bosons comparable with the experiment, $N_b \approx 114$. Ω and U were not changed between the initial and final Hamiltonians. In accordance with the experimental protocol [28], to generate disorder (at the evolution stage) we square a two-dimensional array of random numbers distributed uniformly between 0 and $\delta_{\max}$, for some positive number $\delta_{\max}$, then convolve it with a Gaussian profile with a standard deviation of 0.5. The disorder strength Δ_g is defined as the full width at half maximum of the resulting disorder profile.

The first column in Fig. 1 depicts the evolution of the site occupations in the absence of disorder. In this case, one can see that the particles expand to reach a steady state with no imbalance. When disorder of strength $\Delta_g = 8$ is introduced (second column in Fig. 1), the motion slows considerably and an imbalance remains at the latest time shown. Note that the width of the disorder distribution in this case is the noninteracting bandwidth, $8J$. For very strong disorder ($\Delta_g = 13$, third column in Fig. 1), the particles remain almost entirely in the initially occupied region.

For a more quantitative understanding of the dynamics, in Fig. 2(a) we plot the imbalance $\mathcal{I}$ [defined in Eq. (4)] as a function of time for five values of the disorder strength. For $t < t^*$, the imbalance barely changes. This is an artifact of GMFT for the initial state, which is mostly a Mott insulating domain. Beyond t^*, one can see that $\mathcal{I}$ quickly vanishes in the clean limit and for weak disorder. But as the disorder strength increases it takes longer for $\mathcal{I}$ to reach the expected $\mathcal{I} = 0$ steady state value. The changes in the time evolution are smooth with increasing Δ_g. In Fig. 2(a), we also plot the experimental results taking t^* to be the starting time for the experiments. The GMFT results are qualitatively similar to those in the experiments. They are actually quantitatively similar for weak disorder. As the disorder strength is increased, $\mathcal{I}$ can be seen to exhibit a faster decay in the experiments than within GMFT.

In Fig. 2(b), we plot the imbalance at different times, alongside experimental results [28], as a function of the disorder strength. A common feature seen in both theory and experiment is a transition from zero imbalance (up to fluctuations) to a nonzero imbalance as the disorder strength is increased. Within GMFT we find that the transition point moves to stronger disorder strengths as t increases. A similar trend was seen in experiments for $t \lesssim 200$, but the experimental results appeared to saturate for $200 \lesssim t \lesssim 300$. For any given selected time, the transition point occurs at a smaller value of Δ_g in GMFT when compared to the experiments, which is expected given the slower dynamics of the former seen in Fig. 2(a).

The inverse decay length, λ [Eq. (5)], offers another way to quantify the degree of localization by parameterizing the extent to which disorder suppresses the relaxation of site occupations. The inset in Fig. 2(b) shows λ versus Δ_g for $t = 200$ and the experimental results for $t = 187$. The behavior of λ (inset) is qualitatively similar to that of $\mathcal{I}$ (main panel) in that they both indicate an apparent transition point to a localized regime. Our main finding so far is that the nature of the differences between GMFT and the experiments is quantitative not qualitative.

In general in experiments, and in particular in Ref. [28], Mott insulating states are not at $T = 0$. In order to understand how nonzero temperatures in the initial state modify the dynamics from what we have discussed for $T = 0$, we have done calculations for initial thermal states with $T = 0.33$ and the same Hamiltonian parameters as for $T = 0$. The results obtained for $\mathcal{I}$ and λ are reported in Figs. 2(c) and 2(d). They are qualitatively, and quan-

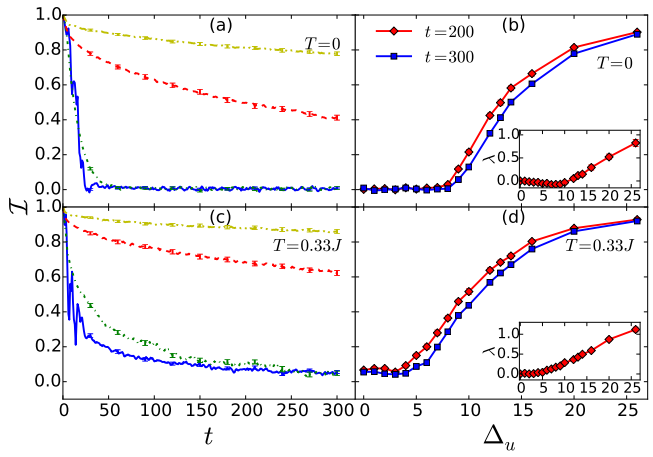

Figure 3. Same as Fig. 2 but for the non-quenched case. The initial state is the ground state of Eq. (1) for $U = 24.4$, $\Omega = 0.145$, and $\mu = 4$ in the presence of uniformly distributed disorder with strength Δ_u. At time $t = 0$ all bosons in the right half of the trap are removed while the remainder are allowed to evolve for $t > 0$. In panels (a) and (c), the lines correspond to $\Delta_u = 0, 4, 13$ and 20 from bottom to top.

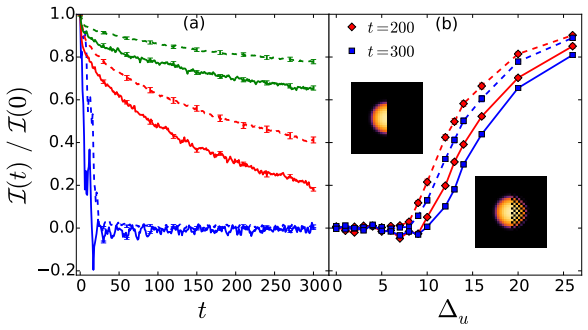

Figure 4. The solid (dashed) lines plot the normalized imbalance where the right half of the trap was initialized to a checkerboard (empty) pattern as shown in the insets. (a) The normalized imbalance against time for various disorder strengths. The pairs of (solid/dashed) lines correspond to $\Delta_u = 0, 13$ and 20 from bottom to top. (b) The normalized imbalance at times $t = 200$ and 300 against disorder strength. The other system parameters are the same as those of Fig. 3.

titatively, similar to those obtained for $T = 0$. The only apparent difference is that t^* is smaller at nonzero temperature than at $T = 0$. This is expected since the Mott insulating domain at nonzero temperature is surrounded by a wider region with a nonvanishing order parameter.

Non-quenched case: In order to understand how the dynamics change if the initial state is not a Mott insulator but rather a superfluid or a Bose-glass, depending on the strength of the disorder, here we consider the dynamics after removing all bosons in one half of the system but without quenching any Hamiltonian parameters (we refer to this protocol as the "non-quenched case"). For this protocol, the initial state is selected to be the ground state for the same values of J, Ω, and U as in the experiment after the quench, but we trap a smaller number of bosons (the site occupations in the center of the trap are still very close to those in the Mott insulating state). Different from the quenched case, here we take the disorder to be distributed uniformly in the interval $[-\Delta_u/2, \Delta_u/2]$, to show that the qualitative results do not depend on the details of the disorder profile.

The evolution of the site occupations is shown in the right panel of Fig. 1, for three values of Δ_u. The first row makes apparent that there are no Mott domains ($n_i < 1$), in contrast to the cases in the left panel. The results during the time evolution are, on the other hand, qualitatively similar in the left and right panels. Localization is seen to occur as the strength of the disorder is increased.

Figure 3(a) shows the time evolution of $\mathcal{I}$ for four values of the strength of the disorder. Comparing Figs. 2(a) and 3(a) one can see that the behavior of the non-quenched and quenched cases is qualitatively similar. Quantitative differences are, on the other hand, apparent. In the non-quenched case there is no t^* such that $\mathcal{I}$ does not change appreciably for $t < t^*$. This is because the order parameter in the non-Mott regime is sizable. In addition, $\mathcal{I}$ decays more quickly in the non-quenched than in the quenched case. This is expected for weak disorder strengths, for which the initial state is superfluid, but it is also the case in the Bose-glass regime present for strong disorder. The results for $\mathcal{I}$ vs Δ_u [Fig. 3(b)] and for λ vs Δ_u [inset in Fig. 3(b)] at different times t are also qualitatively similar to those in Fig. 2(b) and its inset. The transition point to the localized regime increases as t increases. Figs. 3(c) and 3(d) show that the dynamics of the system slows down with the introduction of a nonzero temperature ($T = 0.33$) in the initial state. This is understandable as nonzero temperatures reduce the magnitude of the order parameter in the superfluid and Bose-glass phases [46]. Overall, we find no qualitative change in comparing the quenched and non-quenched cases.

Checkerboard case: As mentioned in the introduction, the initial expansion of bosons in the empty half of the trap in the presence of disorder is expected to be dominated by Anderson physics, due to the low site occupations. In order to test how enhancing interactions by increasing site occupations affects the expansion, we have devised an "improved" version of the initial state considered in the non-quenched case. This "improved" initial state is generated by emptying sites in one half of the system according to a checkerboard pattern (see the insets in Fig. 4). The dynamics then proceeds as in the non-quenched case, by allowing the remaining bosons to evolve without any change in the Hamiltonian parameters. Before emptying sites, the system was in the ground state as in the non-quenched case.

In Figs. 4(a) [4(b)], we plot the normalized imbalance $\mathcal{I}(t)/\mathcal{I}(0)$ against t (Δ_u) for various disorder strengths Δ_u (times t). One can see that the presence of the checkerboard pattern speeds up the decay of $\mathcal{I}(t)/\mathcal{I}(0)$

by enhancing the effect of interactions during the dynamics. It would be interesting to find out how changes in the pattern used for the initial state change the results in the experiments [28].

Discussion: Motivated by the experiments of Ref. [28], we have studied the dynamics of bosons in 2D lattices in the presence of disorder within GMFT. We have shown that GMFT qualitatively describes the experimental findings. We have also shown that the features observed in the experiments are robust for various initial states: Mott insulator, superfluid, and Bose-glass. Since GMFT misses the entanglement present in MBL phases, our results suggest that further experiments will be needed to unambiguously show that MBL is occurring in those systems. Avoiding macroscopic mass transport, as done in Ref. [27], will help rule out slow dynamics due to Anderson and Bose-glass physics.

ACKNOWLEDGMENTS

M.Y., H.H., and V.W.S. acknowledge support from AFOSR (FA9550-15-1-0445) and ARO (W911NF-16-1-0182), and M.R. acknowledges support from the Office of Naval Research. We are grateful to I. Bloch, S. Das Sarma, B. DeMarco, C. Gross, and D. Huse for discussions, and to J. Choi for sending us details about the experimental setup [28].

[1] P. Verkerk, B. Lounis, C. Salomon, C. Cohen-Tannoudji, J.-Y. Courtois, and G. Grynberg, "Dynamics and spatial order of cold cesium atoms in a periodic optical potential," Phys. Rev. Lett. **68**, 3861 (1992).

[2] P. S. Jessen, C. Gerz, P. D. Lett, W. D. Phillips, S. L. Rolston, R. J. C. Spreeuw, and C. I. Westbrook, "Observation of quantized motion of Rb atoms in an optical field," Phys. Rev. Lett. **69**, 49 (1992).

[3] A. Hemmerich and T. W. Hansch, "Two-dimesional atomic crystal bound by light," Phys. Rev. Lett. **70**, 410 (1993).

[4] I. Bloch, J. Dalibard, and W. Zwerger, "Many-body physics with ultracold gases," Rev. Mod. Phys. **80**, 885 (2008).

[5] M. A. Cazalilla, R. Citro, T. Giamarchi, E. Orignac, and M. Rigol, "One dimensional bosons: From condensed matter systems to ultracold gases," Rev. Mod. Phys. **83**, 1405 (2011).

[6] M. Köhl, H. Moritz, T. Stöferle, K. Günter, and T. Esslinger, "Fermionic atoms in a three dimensional optical lattice: Observing Fermi surfaces, dynamics, and interactions," Phys. Rev. Lett. **94**, 080403 (2005).

[7] J. Billy, V. Josse, Z. Zuo, A. Bernard, B. Hambrecht, P. Lugan, D. Clément, L. Sanchez-Palencia, P. Bouyer, and A. Aspect, "Direct observation of Anderson localization of matter waves in a controlled disorder," Nature **453**, 891 (2008).

[8] G. Roati, C. D'Errico, L. Fallani, M. Fattori, C. Fort, M. Zaccanti, G. Modugno, M. Modugno, and M. Inguscio, "Anderson localization of matter waves in a Bose-Einstein condensate," Nature **453**, 895 (2008).

[9] J. Chabé, G. Lemarié, B. Grémaud, D. Delande, P. Szriftgiser, and J. C. Garreau, "Experimental observation of the Anderson metal-insulator transition with atomic matter waves," Phys. Rev. Lett. **101**, 255702 (2008).

[10] G. Lemarié, J. Chabé, P. Szriftgiser, J.C. Garreau, B. Grémaud, and D. Delande, "Observation of the Anderson metal-insulator transition with atomic matter waves: Theory and experiment," Phys. Rev. A **80**, 043626 (2009).

[11] S. S. Kondov, W. R. McGehee, J. J. Zirbel, and B. DeMarco, "Three-dimensional Anderson localization of ultracold matter," Science **334**, 66 (2011).

[12] F. Jendrzejewski, A. Bernard, K. Mulller, P. Cheinet, V. Josse, M. Piraud, L. Pezze, L. Sanchez-Palencia, A. Aspect, and P. Bouyer, "Three-dimensional localization of ultracold atoms in an optical disordered potential," Nat. Phys. **8**, 398 (2012).

[13] M. Greiner, O. Mandel, T. Esslinger, T. W. Hansch, and I. Bloch, "Quantum phase transition from a superfluid to a Mott insulator in a gas of ultracold atoms," Nature **415**, 39 (2002).

[14] T. Stöferle, H. Moritz, C. Schori, M. Köhl, and T. Esslinger, "Transition from a strongly interacting 1d superfluid to a Mott insulator," Phys. Rev. Lett. **92**, 130403 (2004).

[15] I. B. Spielman, W. D. Phillips, and J. V. Porto, "Mott-insulator transition in a two-dimensional atomic Bose gas," Phys. Rev. Lett. **98**, 080404 (2007).

[16] R. Jordens, N. Strohmaier, K. Guenther, H. Moritz, and T. Esslinger, "A Mott insulator of fermionic atoms in an optical lattice," Nature **455**, 204 (2008).

[17] U. Schneider, L. Hackermueller, S. Will, T. Best, I. Bloch, T. A. Costi, R. W. Helmes, D. Rasch, and A. Rosch, "Metallic and insulating phases of repulsively interacting fermions in a 3D optical lattice," Science **322**, 1520 (2008).

[18] Y. P. Chen, J. Hitchcock, D. Dries, M. Junker, C. Welford, and R. G. Hulet, "Phase coherence and superfluid-insulator transition in a disordered Bose-Einstein condensate," Phys. Rev. A **77**, 033632 (2008).

[19] M. White, M. Pasienski, D. McKay, S. Q. Zhou, D. Ceperley, and B. DeMarco, "Strongly interacting bosons in a disordered optical lattice," Phys. Rev. Lett. **102**, 055301 (2009).

[20] M. Pasienski, D. McKay, M. White, and B. DeMarco, "A disordered insulator in an optical lattice," Nat. Phys. **6**, 677 (2010).

[21] B. Gadway, D. Pertot, J. Reeves, M. Vogt, and D. Schneble, "Glassy behavior in a binary atomic mixture," Phys. Rev. Lett. **107**, 145306 (2011).

[22] M. C. Beeler, M. E. W. Reed, T. Hong, and S. L. Rolston, "Disorder-driven loss of phase coherence in a quasi-2D cold atom system," New J. Phys. **14**, 073024 (2012).

[23] J.-P. Brantut, J. Meineke, D. Stadler, S. Krinner, and T. Esslinger, "Conduction of ultracold fermions through a mesoscopic channel," Science **337**, 1069 (2012).

[24] L. Tanzi, E. Lucioni, S. Chaudhuri, L. Gori, A. Kumar,

C. D'Errico, M. Inguscio, and G. Modugno, "Transport of a Bose gas in 1D disordered lattices at the fluid-insulator transition," Phys. Rev. Lett. **111**, 115301 (2013).
[25] S. Krinner, D. Stadler, J. Meineke, J. P. Brantut, and T. Esslinger, "Superfluidity with disorder in a thin film of quantum gas," Phys. Rev. Lett. **110**, 100601 (2013).
[26] S. S. Kondov, W. R. McGehee, W. Xu, and B. DeMarco, "Disorder-induced localization in a strongly correlated atomic Hubbard gas," Phys. Rev. Lett. **114**, 083002 (2015).
[27] M. Schreiber, S. S. Hodgman, P. Bordia, H. P. Lüschen, M. H. Fischer, R. Vosk, E. Altman, U. Schneider, and I. Bloch, "Observation of many-body localization of interacting fermions in a quasirandom optical lattice," Science **349**, 842 (2015).
[28] J.-Y. Choi, S. Hild, J. Zeiher, P. Schaub, A. Rubio-Abadal, T. Yefsah, V. Khemani, D. A. Huse, I. Bloch, and C. Gross, "Exploring the many-body localization transition in two dimensions," (2016), arXiv:1604.04178.
[29] M. P. A. Fisher, P. B. Weichman, G. Grinstein, and D. S. Fisher, "Boson localization and the superfluid-insulator transition," Phys. Rev. B **40**, 546 (1989).
[30] R. T. Scalettar, G. Batrouni, and G. T. Zimanyi, "Localization in interacting, disordered, bose systems," Phys. Rev. Lett. **66**, 3144 (1991).
[31] D. M. Basko, I. L. Aleiner, and B. L. Altshuler, "Metal-insulator transition in a weakly interacting many-electron system with localized single-particle states," Ann. Phys. **321**, 1126 (2006).
[32] V. Oganesyan and D. A. Huse, "Localization of interacting fermions at high temperature," Phys. Rev. B **75**, 155111 (2007).
[33] A. Pal and D.A. Huse, "Many-body localization phase transition," Phys. Rev. B **82**, 174411 (2010).
[34] J. M. Deutsch, "Quantum statistical mechanics in a closed system," Phys. Rev. A **43**, 2046 (1991).
[35] M. Srednicki, "Chaos and quantum thermalization," Phys. Rev. E **50**, 888 (1994).
[36] M. Rigol, V. Dunjko, and M. Olshanii, "Thermalization and its mechanism for generic isolated quantum systems," Nature **452**, 854 (2008).
[37] R. Nandkishore and D. A. Huse, "Many-body localization and thermalization in quantum statistical mechanics," Annu. Rev. Condens. Matter Phys. **6**, 15 (2015).
[38] V. W. Scarola and B. DeMarco, "Dynamics of hubbard-band quasiparticles in disordered optical lattices," Phys. Rev. A **92**, 053628 (2015).
[39] R. Mondaini and M. Rigol, "Many-body localization and thermalization in disordered hubbard chains," Phys. Rev. A **92**, 041601 (2015).
[40] D. S. Rokhsar and B. G. Kotliar, "Gutzwiller projection for bosons," Phys. Rev. B **44**, 10328 (1991).
[41] D. Jaksch, C. Bruder, J. I. Cirac, C. W. Gardiner, and P. Zoller, "Cold bosonic atoms in optical lattices," Phys. Rev. Lett. **81**, 3108 (1998).
[42] I. Hen and M. Rigol, "Superfluid to Mott insulator transition of hardcore bosons in a superlattice," Phys. Rev. B **80**, 134508 (2009).
[43] I. Hen, M. Iskin, and M. Rigol, "Phase diagram of the hard-core Bose-Hubbard model on a checkerboard superlattice," Phys. Rev. B **81**, 064503 (2010).
[44] K. Sheshadri, H. R. Krishnamurthy, R. Pandit, and T. V. Ramakrishnan, "Percolation-enhanced localization in the disordered bosonic Hubbard model," Phys. Rev. Lett. **75**, 4075 (1995).
[45] B. Damski, J. Zakrzewski, L. Santos, P. Zoller, and M. Lewenstein, "Atomic Bose and Anderson glasses in optical lattices," Phys. Rev. Lett. **91**, 080403 (2003).
[46] P. Buonsante, V. Penna, A. Vezzani, and P. B. Blakie, "Mean-field phase diagram of cold lattice bosons in disordered potentials," Phys. Rev. A **76**, 011602 (2007).
[47] P. Buonsante, F. Massel, V. Penna, and A. Vezzani, "Gutzwiller approach to the Bose-Hubbard model with random local impurities," Phys. Rev. A **79**, 013623 (2009).
[48] C. H. Lin, R. Sensarma, K. Sengupta, and S. Das Sarma, "Quantum dynamics of disordered bosons in an optical lattice," Phys. Rev. B **86**, 214207 (2012).
[49] D. Jaksch, V. Venturi, J. I. Cirac, C. J. Williams, and P. Zoller, "Creation of a molecular condensate by dynamically melting a Mott insulator," Phys. Rev. Lett. **89**, 040402 (2002).
[50] J. Zakrzewski, "Mean field dynamics of superfluid-insulator phase transition in a gas of ultra cold atoms," Phys. Rev. A **71**, 043601 (2005).
[51] M. Snoek and W. Hofstetter, "Two-dimensional dynamics of ultracold atoms in optical lattices," Phys. Rev. A **76**, 051603 (2007).
[52] F. A. Wolf, I. Hen, and M. Rigol, "Collapse and revival oscillations as a probe for the tunneling amplitude in an ultracold Bose gas," Phys. Rev. A **82**, 043601 (2010).
[53] M. Snoek, "Rigorous mean-field dynamics of lattice bosons: Quenches from the Mott insulator," Europhys. Lett. **95**, 30006 (2011).
[54] I. Hen and M. Rigol, "Analytical and numerical study of trapped strongly correlated bosons in two- and three-dimensional lattices," Phys. Rev. A **82**, 043634 (2010).
[55] M. Jreissaty, J. Carrasquilla, F. A. Wolf, and M. Rigol, "Expansion of Bose-Hubbard Mott insulators in optical lattices," Phys. Rev. A **84**, 043610 (2011).
[56] M. Yan, H. Y. Hui, and V. W. Scarola, "Dynamics of disordered states in the Bose-Hubbard model with confinement," (2016), arXiv:1601.06817.
[57] B. Bauer and C. Nayak, "Area laws in a many-body localized state and its implications for topological order," J. Stat. Mech: Theory Exp. **2013**, P09005 (2013).
[58] H. Kim and D. A. Huse, "Ballistic spreading of entanglement in a diffusive nonintegrable system," Phys. Rev. Lett. **111**, 127205 (2013).
[59] J. H. Bardarson, F. Pollmann, and J. E. Moore, "Unbounded growth of entanglement in models of many-body localization," Phys. Rev. Lett. **109**, 017202 (2012).